



# White light emission transparent polymer nanocomposites with novel poly(*p*-phenylene vinylene) derivatives and surface functionalized CdSe/ZnS NCs



Bingxin Liu<sup>a</sup>, Xiaodan Lü<sup>a,b</sup>, Chunyu Wang<sup>a,c</sup>, Cuiyan Tong<sup>a,\*</sup>, Yao He<sup>a</sup>, Changli Lü<sup>a,\*</sup>

<sup>a</sup> Institute of Chemistry, Northeast Normal University, Changchun 130024, PR China

<sup>b</sup> Institute of Chemistry, Zhuhai College, Jilin University, Zhuhai 519041, PR China

<sup>c</sup> State Key Laboratory of Supramolecular Structure and Materials, Jilin University, Changchun 130012, PR China

## ARTICLE INFO

### Article history:

Received 6 February 2013

Received in revised form

23 April 2013

Accepted 23 April 2013

Available online 10 May 2013

### Keywords:

White light emission

MEH-PPV derivatives

CdSe/ZnS NCs

Polymer nanocomposites

8-Hydroxyquinoline

Surface functionalization

## ABSTRACT

A series of new polymers with conjugated poly(*p*-phenylene vinylene) units and non-conjugated poly(*p*-xylylene) units containing vinyl and carboxyl groups were synthesized. The monodisperse CdSe/ZnS nanocrystals with a red light emission were prepared by using the phosphine-free precursors. A novel fluorescent polymer and 5-(2-methacryloylethylloxymethyl)-8-quinolinol were dispersed in vinyl monomers containing CdSe/ZnS NCs to successfully fabricate transparent bulk nanocomposites by *in situ* polymerization. The 5-(2-methacryloylethylloxymethyl)-8-quinolinol molecules can be coordinated to the surface of CdSe/ZnS nanocrystals to form a metalloquinolate with green light emission at about 500 nm, while the red light emission of nanocrystals remained after the polymerization process. The efficient white light emitting polymer nanocomposites with color coordinates (0.32, 0.34) can be obtained when the weight ratio of nanocrystals to 5-(2-methacryloylethylloxymethyl)-8-quinolinol is 10:1. A charge transfer from the photoexcited metalloquinolates to the nanocrystals was observed in the system.

© 2013 Elsevier Ltd. All rights reserved.

## 1. Introduction

It is well known that the white light emission can be achieved by mixing and tuning the three primary colors, namely red, green, and blue light or according to the principle of complementary colors, such as blue and yellow light. White light emitting phosphors have drawn much interest since white light emitting diodes (WLEDs) possess numerous advantageous properties such as high brightness, low power consumption and longevity [1]. Semiconductor nanocrystals (NCs), also known as semiconductor Quantum Dots (QDs), have special physical dimensions [2–6] and have many potential applications in the fields of electro-optical devices [7,8], sensors [9], and biological labeling [10]. To give these functional composite NCs a good processability, the NCs can be integrated into some flexible matrices. More importantly, we can combine the desired properties from both components in one, thus creating the new properties that may not be present in each individual material. However, the transparency of the resultant nanocomposites apparently drops when a high content of NCs needs to be integrated into the polymer matrix due to scattering from large particles or agglomerates. Some synthetic techniques have been investigated to

prevent aggregation of QDs during the polymerization process. Zhang's group utilized the polymerizable surfactant to transfer single-colored CdTe to styrene or PPV precursor to obtain a solid polymer composite [11]. Lee et al. used phosphine ligand covered QDs to prevent the QDs from phase separating during polymerization [12]. Pang et al. presented a novel method to fabricate the PMMA-CdSe/ZnS composites by pre-polymerization [13]. Our research group prepared a series of functionalized ZnS NPs/polymer transparent nanocomposites with high NPs content by *in situ* bulk polymerization [14,15]. ZnS:Mn [16], ZnO [17], and other NCs still were blended into some flexible matrix. These obtained fluorescent nanocomposites have attracted much interest for their promising potential in the fields such as electroluminescent and optoelectronic devices.

Since poly(*p*-phenylene vinylene) (PPV) as the first electroluminescence material was discovered in 1990 [18], PPV and their derivatives have become the most classical conjugated polymers used in polymer light-emitting diodes (PLEDs), solar cells, and biosensors [19–21]. Especially, poly(2-methoxy-5-(2'-ethylhexyloxy)-*p*-phenylene vinylene) (MEH-PPV) has attracted much attention due to its relatively good solubility and easy processability [22,23]. In recent years, in order to satisfy various uses, some functional groups were incorporated into the backbone chain or the side chain of PPV and their derivatives [24–27]. Multifarious functional groups such as vinyl

\* Corresponding authors. Fax: +86 43185098768.

E-mail address: [lucl055@nenu.edu.cn](mailto:lucl055@nenu.edu.cn) (C. Lü).

groups, propynylphenyl groups, methacrylate groups, ATRP initiator groups, dithiocarbamate initiator groups and propargyl groups can be grafted to the PPV-copolymer by esterification process or “click” chemistry reaction [28–30]. Unfortunately, precious metals such as Pt or Pd derivative were usually used as catalyst. So generally speaking, the cost of these reactions is much higher. The water solubility of PPV derivatives is generally achieved by attaching hydrophilic charged units, such as carboxylate, phosphonate, and sulfonate groups (anionic) or tertiary ammonium groups (cationic) onto side chains of the polymer [31]. These reactions either generally required longer reaction time or employed harmful or noxious reagents.

In this paper, the novel conjugated/non-conjugated polymer consisting of MEH-PPV,  $\alpha$ -(4-vinylbenzyl)-thiomethyl- $\alpha'$ -carboxyl-2-methoxy-5-(2'-ethylhexyloxy)-*p*-phenyleneethylene moieties (VBCPPX) and  $\alpha$ -(4-vinylbenzyl)-thiomethyl-2-methoxy-5-(2'-ethylhexyloxy)-*p*-phenylene-xylene moieties (VBPPX) was synthesized via a typical chlorine precursor route and a similar addition reaction by *S*-(4-vinyl)-benzylisothiurea hydrochloride (SVBTC). The CdSe/ZnS core-shell NCs with red light emission were also synthesized by high-temperature implantation method. The new fluorescent polymer (S-1.5) and 5-(2-methacryloylethylloxymethyl)-8-quinolinol (MQ) were also introduced into the vinyl monomers containing CdSe/ZnS NCs to prepare a series of transparent bulk nanocomposites with good fluorescent properties by *in situ* polymerization route (see Scheme 1). The vinyl group on the side chain of the new polymer can copolymerize with MQ and vinyl monomers such as styrene. The MQ molecules can coordinate with Zn<sup>2+</sup> on the surface of CdSe/ZnS NCs to form a metal complex with green light emission by a ligand exchange process. There are the covalent bonds between MQ decorated NCs and polymer matrix by double bonds of MQ, which could improve the compatibility between the NCs and polymers, and impart the resultant bulk nanocomposites with high transparency and stable fluorescent emission as well as an excellent thermal stability. This strategy can provide a facile route for the fabrication of white light emitting polymer bulk nanocomposites by adjusting the content of different emission components. The white light emission is originated

from the trichromatic superposition of the emission of MEH-PPV derivative (blue), emission of CdSe/ZnS NCs (red) and the surface-coordination emission (green) of the metal complex of MQ units on NCs. The structure and optical properties of the novel MEH-PPV derivatives and polymer nanocomposites were studied in detail.

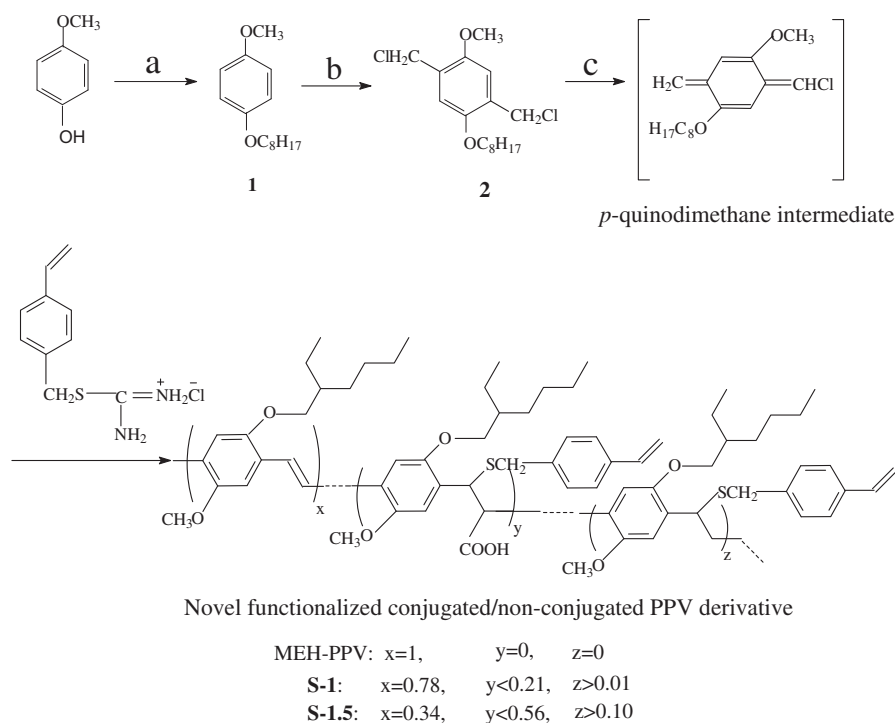
## 2. Experimental section

### 2.1. Materials

2-Ethylhexyl bromide (95%) was purchased from Acros. Divinylbenzene (DVB, 80%) was purchased from Aldrich. *N,N*-dimethylacrylamide (DMAA) was obtained from TCI. Styrene was distilled under reduced pressure before use. 1,4-Dioxane was purified by distillation in the presence of sodium and stored over silica gel-self indicator. 2,2'-Azobisisobutyronitrile (AIBN) was recrystallized in ethanol. *tert*-BuOK was freshly prepared by reaction of *tert*-BuOH with potassium. 4-Vinylbenzyl chloride (90%) was purchased from Fluka. Cadmium oxide (CdO, 99.99%), sulfur (S, 99.98%, powder), 1-octadecene (ODE, 90%), oleic acid (OA, 90%), selenium (Se, 99.99%, powder), zinc oxide (ZnO, 99.99% powder), and octadecylamine (ODA) were purchased from Aldrich. 4-Methoxyphenol, thiourea, tetrabutyl ammonium bromide (TBABr) and other chemical reagents were used as received without purification.

### 2.2. Synthesis of methoxy-4-(2-ethylhexyloxy)benzene (1) [32]

To a stirred mixture of 4-methoxyphenol (10.0 g, 81 mmol), KOH (5.6 g, 0.1 mol), TBABr (0.5 g, 17 mmol) and water (30 mL) was added 2-ethylhexyl bromide (15.4 g, 80 mmol). The reaction was then heated to reflux for 3 days under N<sub>2</sub> atmosphere. After waiting for the solution to cool room temperature, the resulting mixture was extracted with diethyl ether (150 mL) and the organic layer was washed with sodium hydroxide (100 mL 0.5 M) and water (100 mL) respectively, then dried over anhydrous Na<sub>2</sub>SO<sub>4</sub> and



**Scheme 1.** Synthetic route of the novel conjugated/non-conjugated polymer: (a) 2-Ethylhexyl bromide, KOH, TBABr, H<sub>2</sub>O, N<sub>2</sub>, reflux, 3d; (b) HCHO, HCl, 1,4-dioxane, 90 °C, 72 h; (c) SVBTC, *tert*-BuOK, 1,4-dioxane, N<sub>2</sub>, 60 °C, 4 h.

finally, diethyl ether was eliminated in vacuo. The crude product was purified by column chromatography [silica gel; petroleum ether/diethyl ether (3:1) as an eluent]. The light yellow liquid product **1** (14.9 g) was obtained by vacuum distillation method (78% yield).  $^1\text{H}$  NMR (500 MHz,  $\text{CDCl}_3$ ,  $\delta$ ): 6.84 (s, 4H, aromatic H), 3.8 (s, 2H,  $-\text{OCH}_2-$ ), 3.78 (s, 3H,  $-\text{OCH}_3$ ), 0.9–1.7 (m, 15H).

### 2.3. Synthesis of 1,4-bis(chloromethyl)-5-(2-ethylhexyloxy)-2-methoxybenzene (**2**) [33,34]

Compound **2** was synthesized by reacting compound **1** (10 g, 43 mmol) with formaldehyde (20 g, 0.67 mol) and concentrated hydrochloric acid (40 mL) in 1,4-dioxane (30 mL). After the solution was heated at 90 °C for 3 days, the ethyl acetate and water were added into the reaction mixture when it cooled to ambient temperature. After the precipitation was filtrated, the crude solid was dissolved in a small amount of hot cyclohexane and then poured the solution into ice-cold methanol. The white solid was obtained after filtration and vacuum drying (6.06 g, 43% yield, mp 47–48 °C).  $^1\text{H}$  NMR (500 MHz,  $\text{CDCl}_3$ ,  $\delta$ ): 6.92 (d, 2H, aromatic H), 4.64 (s, 4H,  $-\text{CH}_2\text{Cl}$ ), 3.88 (d, 2H,  $-\text{OCH}_2-$ ), 3.86 (s, 3H,  $-\text{OCH}_3$ ), 0.9–1.75 (m, 15H).

### 2.4. Synthesis of S-(4-vinyl)-benzyl isothiurea hydrochloride (**SVBTC**) [35]

15.3 g of 4-vinylbenzyl chloride (0.1 mol), 9.12 g of thiourea (0.12 mol), 200 mL of ethanol and 0.08 g of 4-methoxyphenol as inhibitor were put into a three-necked flask fitted with a reflux condenser. The reaction mixture was stirred at reflux temperature for 4 h under  $\text{N}_2$  flow. Then the resulting solution cooled to ambient temperature and was concentrated at a reduced pressure. The survival was poured into a large amount of diethyl ether and the white precipitate was collected and thoroughly washed several times with diethyl ether, and then dried in vacuum.  $^1\text{H}$  NMR (500 MHz,  $\text{D}_2\text{O}$ ,  $\delta$ ): 7.30 (d, 2H, aromatic H), 7.23 (d, 2H, aromatic H), 6.57 (q, 1H,  $-\text{CH}=\text{}$ ), 5.67 (d, 1H,  $=\text{CH}_2$ ), 5.13 (d, 1H,  $=\text{CH}_2$ ), 4.19 (s, 2H,  $-\text{CH}_2\text{S}-$ ).

### 2.5. Synthesis of MEH-PPV

To a round-bottom flask were added 3.5 g of *tert*-BuOK, 20 mL of dry 1,4-dioxane. Under  $\text{N}_2$  atmosphere, a solution of compound **2** (1.0 g) in dry 1,4-dioxane (10 mL) was dropped into the above flask. During this procedure, the solution gradually turned from colorless to orange. The reaction mixture was stirred at 60 °C for 4 h, then cooled to room temperature and poured into a large amount of methanol. Further purification was effected by re-precipitation from  $\text{CHCl}_3/\text{MeOH}$  and dried in vacuo.

### 2.6. Synthesis of the novel polymers

Under  $\text{N}_2$  atmosphere and vigorous stirring, a solution of compound **2** (1.0 g) in dry 1,4-dioxane (10 mL) was dropped into a solution of *tert*-BuOK (3.5 g), and varying weight of **SVBTC** in dry 1,4-dioxane (20 mL). The reaction temperature was maintained at 60 °C for 4 h and then cooled to room temperature. The precipitate was collected after pouring the reaction solution into a large amount of methanol. It was further purified by re-precipitating from  $\text{CHCl}_3/\text{MeOH}$  and dried in vacuo. By using 0.65 g or 0.975 g of **SVBTC**, two kinds of novel polymers defined as **S-1** or **S-1.5** can be obtained, respectively.

### 2.7. Synthesis of the CdSe/ZnS core-shell NCs

The CdSe core was synthesized following traditional methods by using oleic acid (OA) as the capping agents [36]. The concentration of the CdSe QD core was then calculated using the size dependent

extinction coefficient [37]. Next, ZnS shells were deposited in a layer-by-layer fashion via the SILAR method [38]. In a typical synthesis of CdSe/ZnS core-shell NCs, 3 mL of ODE and 0.1 g of ODA were loaded into a 50 mL reaction flask, the purified CdSe NCs in hexanes were added, and the system was kept at 100 °C under nitrogen flow for 30 min to remove hexanes with low vapor pressure. Subsequently, the solution was heated to 220 °C for the shell growth. The sulfur precursor and zinc precursor were injected sequentially, allowing a minimum of 10 min between injections to allow for shell annealing. The process was repeated until a desired thickness was grown.

### 2.8. Preparation of polymer bulk nanocomposites

The CdSe/ZnS NCs, **S-1.5** and MQ were dispersed in monomer mixtures of DMAA, St and DVB. The weight ratio of DMAA/St/DVB was fixed to be 1:5:0.3. Subsequently, 3% w/w of AIBN was added to the above transparent dispersion, and the pre-polymerization was carried out at 75 °C for 15 min after degassing. Then, the polymerization systems were cured at 45 °C for 12 h, followed by a programmed heating process from 50 to 110 °C (at 10 °C/h) and then held at 120 °C for 3 h. Finally, a series of transparent nanocomposites were obtained. The polymer bulk materials with CdSe/ZnS NCs or **S-1.5** were defined as P-QD and P-PPV, respectively. Polymer bulk materials containing CdSe/ZnS NCs and **S-1.5** (1:1, w/w) were simply defined as P-NCs-PPV. The synthetic recipes of P-NCs/MQ-PPV with different dosages of CdSe/ZnS NCs, **S-1.5** and MQ were shown in Table S1.

### 2.9. Characterization

FTIR spectra were recorded on a Magna 560 FT-IR spectrometer. NMR spectra were obtained from an AVANCE Bruker spectrometer at basic frequencies of 500 MHz for  $^1\text{H}$  and 125 MHz for  $^{13}\text{C}$  in  $\text{CDCl}_3$  solution. UV-vis absorption spectra were recorded on a Vary 500 UV-vis-NIR spectrometer in the range 200–800 nm. The photoluminescence properties were measured on a Cary 500 fluorescence spectrometer. The molecular weights of polymers were estimated at a flow rate of 1.0 mL  $\text{min}^{-1}$  at 25 °C by gel permeation chromatography (GPC) on a Waters instrument (Waters Corporation, USA), using  $\text{CHCl}_3$  as eluent, and the molecular weights were determined vs polystyrene standards. X-ray diffraction (XRD) patterns were measured using a Rigaku D/max-II B X-ray diffractometer at a scanning rate of 6°  $\text{min}^{-1}$  with  $2\theta$  ranging from 5° to 80°, using  $\text{CuK}\alpha$  radiation ( $\lambda = 1.5418 \text{ \AA}$ ). Transmission electron microscopy (TEM) was carried out on a JEM-2100F microscope. Thermogravimetric analysis (TGA) was performed on a Perkin Elmer TGA-2 thermogravimetric analyzer under air atmosphere at a heating rate of 10 °C  $\text{min}^{-1}$ .

## 3. Results and discussion

### 3.1. Synthesis and characterization of novel polymers

The preparation process of the novel polymer is illustrated in Scheme 1. The polymerization reaction occurs between compound **2** and **SVBTC** in the presence of *tert*-BuOK via *p*-quinodimethane intermediate as the actual monomer. The S–C bond of **SVBTC** is polarized under the strongly basic conditions and it attacks the active intermediate and induces the polymerization reaction of PPV and eventually generates the novel polymer with the styrene group and carboxyl group in the side chains. The PPV and PPX units are possibly randomly arranged in the main chain of the polymers. The obtained polymers have excellent solubility in  $\text{CHCl}_3$  and THF. The color of the polymers gradually becomes lighter from red to

yellow with increasing amount of **SVBTC** in the polymerization reaction.

Fig. 1 shows the FTIR spectra of MEH-PPV and **S-1.5**. The bands at 3056 and 966  $\text{cm}^{-1}$  are assigned to the olefinic C–H stretching and trans-substituted olefinic C–H bending of MEH-PPV, respectively [39]. The absorptions at 2956, 2925, 2859, 1460, and 1352  $\text{cm}^{-1}$  are assigned to the  $-\text{CH}_2-$  and  $-\text{CH}_3$  groups of side chains. The bands at 1600 and 1503  $\text{cm}^{-1}$  are characteristic of the benzene ring. The absorption band associated with the C–O single bond is at 1203  $\text{cm}^{-1}$  related to the phenyl-oxygen stretch which is the strongest absorption band for MEH-PPV [40]. However, some new strong absorption bands emerge in the novel polymer. For **S-1.5**, the broad peak at 3430  $\text{cm}^{-1}$  is attributed to the bond of O–H. The C=O stretching vibration appears at around 1643  $\text{cm}^{-1}$ , and this peak overlaps with the stretching band of C=C double bond of MEH-PPV units, but the intensity of this band for **S-1.5** is stronger than that of  $-\text{CH}_2-$  and  $-\text{CH}_3$  groups at 2925  $\text{cm}^{-1}$  when compared with that of pure MEH-PPV. These results indicate that the carboxyl group has been successfully incorporated into the side chain of MEH-PPV derivative. The low absorption frequency for the C=O stretching vibration indicates that carboxylic acid groups participate in intramolecular hydrogen bonding [41]. The peak at 1110  $\text{cm}^{-1}$  is attributed to C–O stretching in carboxylic acid [42]. The weakness of absorption for C–S lead to it does not be observed in the FTIR spectra.

The structure and composition of the obtained polymers were determined by NMR spectra (see Table 1). Systematic NMR spectroscopy investigation was carried out via  $^1\text{H}$ ,  $^{13}\text{C}$  NMR, DEPT135, COSY and HMBC spectra together with HMQC techniques. Through the analysis of  $^{13}\text{C}$  NMR and  $^{13}\text{C}$ -DEPT135 spectra in Figs. S1 and S2, it was established that there were 23 species of carbon atoms in **S-1.5**, including 5 quaternary carbon, 8 methine, 7 methylene and 3 methyl group C atoms. Fig. 2 is the representative  $^1\text{H}$  NMR spectrum of **S-1.5** in  $\text{CDCl}_3$ . The peak at 0.88 ppm (region a) belongs to the  $-\text{CH}_3$  of the ethylhexyloxy substituent. The resonance at 1.29–1.64 ppm belongs to the methylene and methenyl groups for ethylhexyloxy substitute [43]. The peaks at 7.0 ppm and 7.25 ppm are assigned to the hydrogen atom of benzene rings. The resonances at 6.61 ppm, 5.66 ppm and 5.17 ppm are attributed to  $-\text{CH}=\text{}$  and  $\text{CH}_2=\text{}$  groups of vinyl benzene [44]. The resonance at 5.17 ppm is represented with region b. Fig. S3 shows the  $^1\text{H}$ - $^{13}\text{C}$  heteronuclear multiple quantum correlation (HMQC) spectrum. There is no detectable resonance peak at 4.57 ppm coupled to  $^{13}\text{C}$  correlation spectrum. However, it has a small resonance peak which is coupled to the carbon as that at 152 ppm (C-w) in the heteronuclear

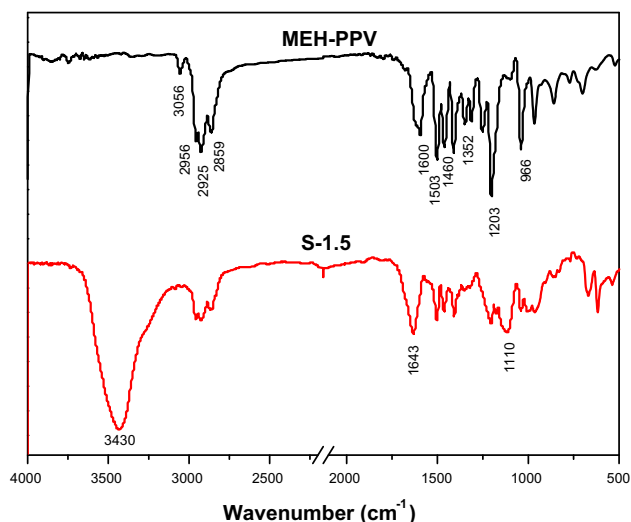


Fig. 1. FTIR spectra of MEH-PPV and **S-1.5**.

Table 1

Properties of the novel conjugated/non-conjugated PPV derivatives synthesized from the polymerization by changing the amounts of **SVBTC**.

Samples	<b>SVBTC</b> / compound 2 (mol) <sup>a</sup>	St units content (mol%) <sup>b</sup>	Carboxyl units content (mol%) <sup>c</sup>	$M_n^d$	PD <sup>e</sup>	Absorp- tion peaks (nm) <sup>f</sup>	Emission peaks (nm) <sup>g</sup>
MEH-PPV	0	—	—	$2.63 \times 10^4$	3.7	489	562
<b>S-1</b>	1	22	21	$1.50 \times 10^4$	3.2	470	528
<b>S-1.5</b>	1.5	66	56	$7.21 \times 10^3$	2.5	360	438 (503 <sup>h</sup> )

<sup>a</sup> Molar ratio of **SVBTC** and Compound 2.

<sup>b</sup> Molar content of styrene units in the polymers calculated by equation (1).

<sup>c</sup> Molar content of carboxyl units in the polymers calculated by equation (2).

<sup>d</sup> Number-average molecular weight.

<sup>e</sup> Polydispersity index ( $M_w/M_n$ ).

<sup>f</sup> Absorption peaks of the polymers in  $\text{CHCl}_3$  with a concentration of 0.01 mg/mL.

<sup>g</sup> Emission peaks of the polymers in  $\text{CHCl}_3$  with a concentration of 0.01 mg/mL.

<sup>h</sup> Emission peaks of **S-1.5** in 0.2 N NaOH (aq) with a concentration of 0.01 mg/mL.

multiple bond correlation (HMBC) spectrum (see Fig. S4). These data indicate that there is no carbon directly attached to this H atom. In other words, the H atom at 4.57 ppm is an active hydrogen. Simultaneously it can be notarized that C-w is a quaternary carbon from  $^{13}\text{C}$  NMR and  $^{13}\text{C}$ -DEPT135 spectra (see Figs. S2 and S3). The characteristic absorption peaks for the groups of  $-\text{OH}$  and  $\text{C}=\text{O}$  are also observed in FTIR spectra. So, we can infer that the peak at 4.57 ppm (region c) belongs to  $-\text{COOH}$  group via the analysis of FTIR and NMR. Because some H atom of  $-\text{COOH}$  group is proton exchanged by H which comes from  $\text{H}_2\text{O}$  in  $\text{CDCl}_3$ , so the sign intensity of HMBC spectrum is very weak and the chemical shift of  $-\text{COOH}$  group moves upfield. The resonances at 2.5–4.0 ppm is assigned to the  $-\text{OCH}_3$ ,  $-\text{OCH}_2-$ ,  $-\text{SCH}_2-$  groups and methenyl groups of PPX unit. But these signals in this region overlap mutually and it is hard to distinguish them by NMR spectra. The complete assignment on  $^1\text{H}$  and  $^{13}\text{C}$  NMR of **S-1.5** was obtained by combining with 2D NMR studies, and the results are listed in Table S2. We presume that the structures of MEH-PPV and PPX units in the polymer are the same as in their homopolymers, and the molar content of styrene units and carboxyl units in the polymers can be calculated by the following equations [45]:

$$\text{Styrene\%} = [6I_b/I_a] \times 100\% \quad (1)$$

$$\text{Carboxyl\%} = [6I_c/I_a] \times 100\% \quad (2)$$

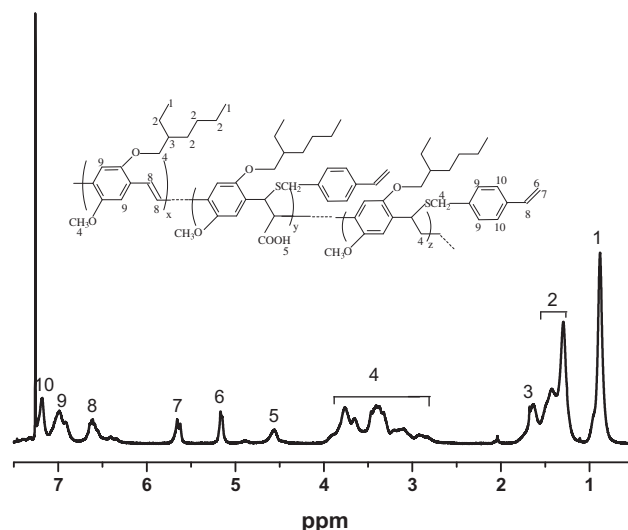


Fig. 2.  $^1\text{H}$  NMR spectrum of **S-1.5**.

where  $I_a$ ,  $I_b$  and  $I_c$  represent the peak integrals in the region **a**, **b** and **c**, respectively. The calculated results are listed in Table 1. It can be seen that the content of styrene units and carboxyl units in the polymers increase with increasing amounts of **SVBTC**. The styrene unit content for **S-1** and **S-1.5** come up to 22% and 66%, respectively. The carboxyl unit contents for **S-1** and **S-1.5** also reach 21% and 56%, respectively. Because of the high content of the two functional groups, the fluorescent conjugated polymer is endowed with greater reactivity. The increase of the molar ratio for the two units in the polymers is not linear with the addition of **SVBTC**. Meanwhile, the ratio between the carboxyl units and styrene units decreases from 0.95 to 0.85 with increasing amounts of **SVBTC**. It should be noted that there is a peak integral for a trace of  $H_2O$  from  $CDCl_3$  in region **c**, so the actual content of carboxyl unit is slightly smaller than the calculation value. The solubility of the novel polymer in polar solvents may be improved by incorporating so many carboxyl groups. It is noteworthy that, **S-1.5** can be dispersed in alkaline aqueous solution. This further indicated that the carboxyl group is incorporated into the novel polymer.

It is known that the conjugation length in an organic conjugated system influences the band gap from HOMO to LUMO. Generally speaking, a shorter conjugation length makes a larger band gap. Therefore, when a non-conjugated segment is incorporated into a conjugated chain, the conjugation structure will be interrupted, and the luminescence emission of the resultant polymer will blue-shift. The luminescence properties of the polymers can be controlled by the incorporated content of PPX unit in the novel polymer. Figs. 3 and 4 show the UV–vis absorption and photoluminescence (PL) spectra of pure MEH-PPV and the novel polymers in  $CHCl_3$  with a concentration of 0.01 mg/mL. The maximum absorption peaks for the three samples can be observed at 489, 470, and 360 nm, respectively. In addition, there is a shoulder peak assigned to B band absorption of the aryl ring at around 300 nm for **S-1** and **S-1.5**. From the spectra, it can be found that the maximum absorption peak exhibits an obvious blue-shift. Generally, the absorption band in UV–vis spectrum correlates to the conjugated structure of the polymer chain. Introduction of non-conjugated segments into conjugated polymer backbones results in the confinement of  $\pi$  electrons in the conjugated fragment. Thus the HOMO–LUMO band gap can be efficiently tailored by the addition of **SVBTC**. The emission properties of the polymers are in accordance with their UV–vis absorption behavior. The maximum emission peaks of MEH-PPV, **S-1** and **S-1.5** appear at 562, 528 and 438 nm, respectively. There is an obvious blue-shift for the emission spectra of the polymers with increasing **SVBTC** content. **S-1.5** can be

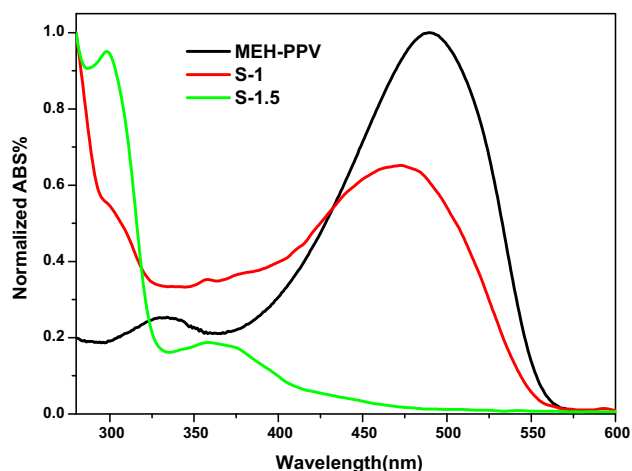


Fig. 3. UV–vis absorption spectra of MEH-PPV, **S-1** and **S-1.5**.

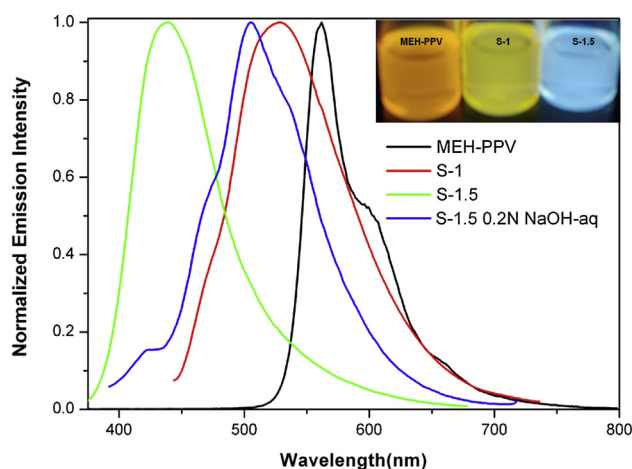


Fig. 4. PL spectra of MEH-PPV, **S-1** and **S-1.5**. Inset: PL photographs of MEH-PPV, **S-1** and **S-1.5** excited by an ultraviolet lamp at 365 nm.

dispersed in water under basic conditions. In Fig. 4, it can be seen that the maximum emission peak of **S-1.5** in 0.2 N NaOH aqueous solutions appears at 503 nm. The peak has an obvious red-shift compared to the one in  $CHCl_3$ . This phenomenon was observed in other PPV derivatives containing carboxyl groups [46]. The inset in Fig. 4 presents the PL optical images of MEH-PPV, **S-1** and **S-1.5** with a concentration of 0.05 mg/mL in  $CHCl_3$  under excitation at 365 nm with a UV lamp. It can be seen that the colors of the MEH-PPV, **S-1** and **S-1.5** change from orange to blue under photoexcitation.

### 3.2. Transparent polymer bulk nanocomposites

Highly monodisperse CdSe/ZnS core–shell NCs have been synthesized by a high-temperature implantation method and OA was used as ligand to avoid widely used phosphine precursors. The TEM images of CdSe core and CdSe/ZnS NCs are shown in Fig. 5. The CdSe core with a diameter of 3.6 nm and CdSe/ZnS NCs with a diameter of 4.7 nm are uniformly distributed without aggregation. The CdSe/ZnS NCs and **S-1.5** were transferred into the organic monomers with different ratios of MQ, followed by *in situ* bulk polymerization to obtain a series of transparent luminescent nanocomposites (Scheme 2). The DMAA is used as the copolymerization monomer to increase the solubility of **S-1.5** in styrene. Because the polymer **S-1.5** has a low solubility (1 mg/g) and low double bond content on the side chain, 5 wt% DVB is also used as the crosslinking agent. Here, the MQ molecules are used as both the copolymerization monomer and the ligand that can coordinate on the surface of CdSe/ZnS NCs to form the metal complexes (ZnMQ) with a green light emission [14]. Here, the **S-1.5** has a blue light emission and the inherent red light emission of CdSe/ZnS NCs may remain in the polymers. Therefore, we were eager to get the white light emission nanocomposites by regulating the proper proportion of MQ in the polymers.

Fig. 6 presents the XRD patterns of CdSe/ZnS NCs, P-NCs/MQ(10:1)-PPV and P-NCs/MQ(2:1)-PPV. It can be seen that the CdSe/ZnS NCs have three strong diffraction patterns at  $2\theta = 28.5^\circ$ ,  $47.5^\circ$  and  $56.3^\circ$  corresponding to the (111), (220), and (311) planes of the standard zinc blende structure of ZnS. This result indicated that the ZnS layers were successfully coated on the surface of CdSe core. However, we did not observe these diffraction patterns in the nanocomposite samples probably due to the low content (0.4 wt%) of CdSe/ZnS NCs in polymer matrix. Fig. 7 shows the FR-IR spectra of P-NCs-PPV, P-NCs/MQ(10:1)-PPV and P-NCs/MQ(2:1)-PPV. The peaks at  $1510$  and  $1550\text{ cm}^{-1}$  are attributed to the C–N stretching vibration of the pyridine rings and the C–C stretching vibration on

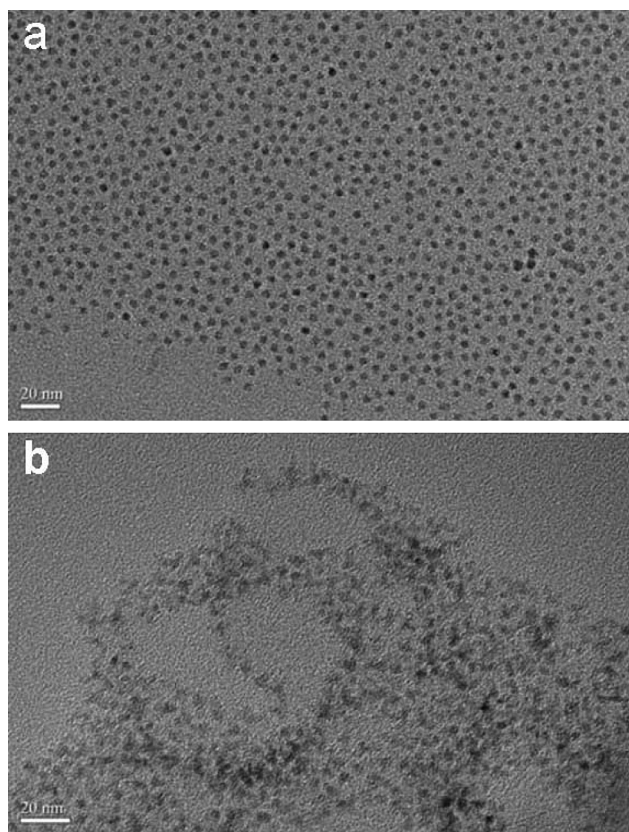


Fig. 5. TEM images of CdSe core (a) and CdSe/ZnS NCs (b).

quinoline rings of MQ units [47]. The intensities of the two peaks in P-NCs/MQ(10:1)-PPV and P-NCs/MQ(2:1)-PPV markedly enhance with the increasing MQ content in polymers as compared with that of the sample of P-NCs-PPV, indicating that the MQ units have been introduced into the nanocomposites.

Fig. 8 is the PL spectra of CdSe/ZnS NCs and S-1.5 in chloroform and polymer nanocomposites, respectively. The CdSe/ZnS NCs in

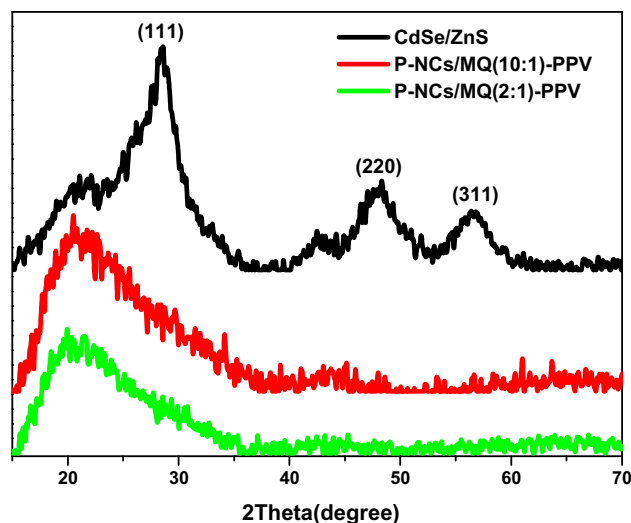


Fig. 6. XRD patterns of CdSe/ZnS NCs, P-NCs/MQ(10:1)-PPV and P-NCs/MQ(2:1)-PPV.

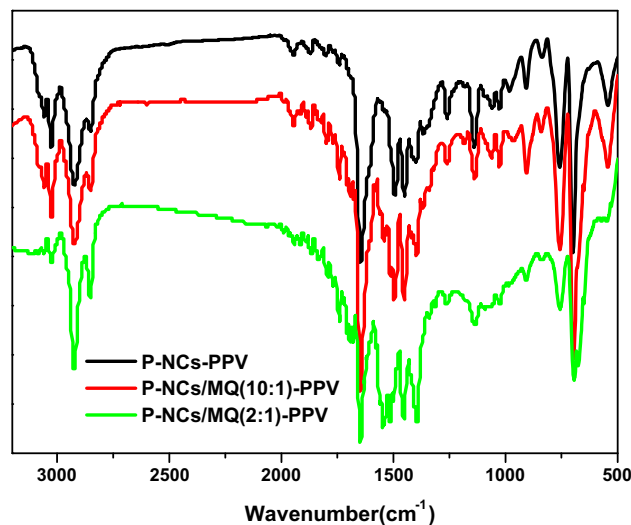
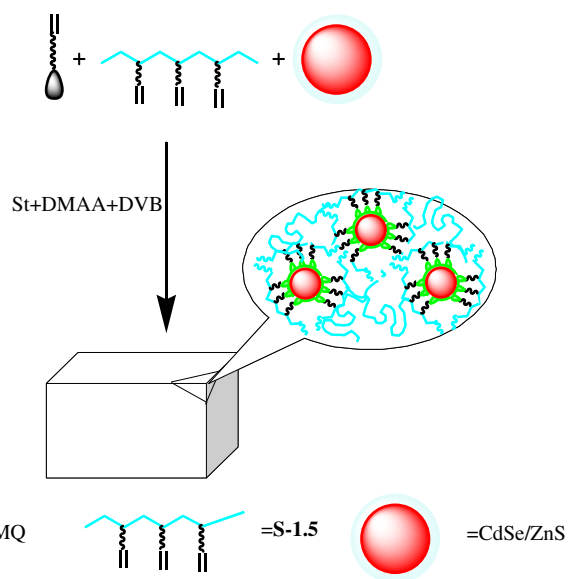


Fig. 7. FTIR spectra of P-NCs-PPV, P-NCs/MQ(10:1)-PPV and P-NCs/MQ(2:1)-PPV.



Scheme 2. Schematic illustration for the preparation of fluorescent polymer nanocomposites with MQ-functionalized CdSe/ZnS NCs and new MEH-PPV derivatives via *in situ* bulk polymerization.

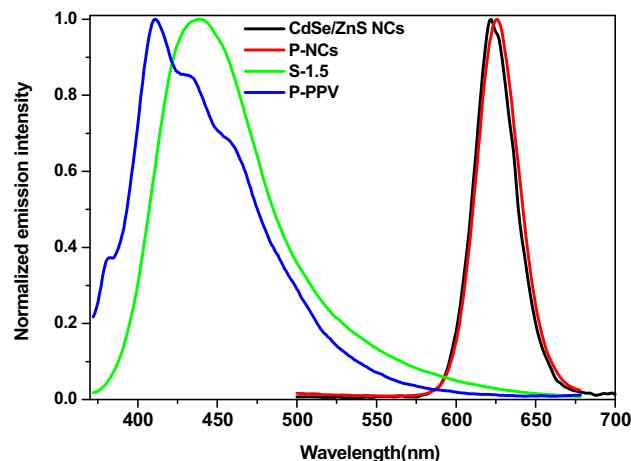


Fig. 8. PL spectra of P-NCs, P-PPV, CdSe/ZnS NCs and S-1.5. Samples of CdSe/ZnS NCs and S-1.5 are in chloroform and the concentration is 0.01 mg/mL.

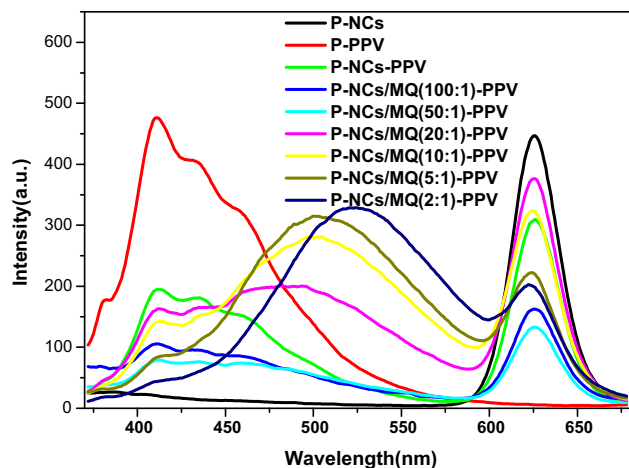


Fig. 9. PL spectra of P-NCs, P-PPV, P-NCs-PPV and different nanocomposites with NCs, S-1.5 and MQ ligands.

chloroform shows a sharp emission peak at 622 nm which slightly red-shifts to 625 nm in bulk nanocomposites (P-NCs). S-1.5 has a sharp PL peak at 438 nm in chloroform and this emission peak blue-shifts to 411 nm in P-NCs because the reaction of S-1.5 and AIBN shortens the conjugation length [25]. A new broad PL peak at 500 nm is observed with the addition of MQ and its intensity increases with the increasing dosage of MQ (Fig. 9), indicating that the MQ units in polymers have coordinated to the surface zinc atoms of NCs to form the fluorescent metalloquinolates [14]. Our previous work has demonstrated that the similar metalloquinolates formed on NCs should be the single coordination type of complex (ZnMQ) because of the steric hindrance effect provided by the special spherical surface of NCs and the existence of Zn–S bonds on the shell of NCs as compared with the conventional coordination compounds such as  $Znq_2$  [1,14]. In addition, the center of the new broad emission peak of the metalloquinolates red-shifts with the increasing dosage of MQ. This phenomenon was observed in the previous study [14] and may be due to the energy transfer or electronic coupling effect between the CdSe/ZnS NCs and the new ZnMQ complexes on NCs [48].

It is well known that the inorganic nanoparticles are prone to aggregation in polymer matrix due to their high specific surface energies and inherently hydrophilic character as well as the compatibility between the nanoparticles and polymers. So, when the nanoparticles are integrated into the polymer matrix, the transparency of the resultant nanocomposites usually drops. Up to

now, the preparation of transparent bulk nanocomposites with uniformly dispersed nanoparticles was still a challenging task [49,50]. In this work, the TEM study was not performed because the content of CdSe/ZnS NCs is very low, and it would be hard to observe the morphology of NCs in the polymer matrix. However, the fluorescent bulk nanocomposites obtained by our strategy are transparent. Fig. 10 shows the PL digital images of the corresponding samples under daylight and excitation at 365 nm with a UV lamp. This result indirectly indicates that the NCs are uniformly distributed in the polymer matrix without phase separation. The pure polymer matrix (P) obtained from the monomer mixture of DMAA/St/DVB presents a blue emission at 473 nm. This weak blue emission band of polymer may be from the contribution of P(DMAA) segments as reported previously [14]. The polymer sample with PPV (P-PPV) exhibits a strong blue light emission while the sample containing NCs (P-NCs-PPV) emit a red light. The pink light emitted P-NCs-PPV can be obtained when the weight ratio of NCs and S-1.5 in the polymer matrix is 1:1. Upon addition of MQ into the polymer matrix, the pink emission turns to green light which is attributed to the cooperative interaction of light emission between different components including PPV derivatives, CdSe/ZnS NCs and the metal complex formed on the NCs. In particular, when the ratio of MQ and NCs reaches 10:1, a nanocomposite with white light emission can be achieved. It is noteworthy from Fig. 11 that the chromaticity coordinate (0.32, 0.34) of this bulk nanocomposite containing NCs, MQ and PPV falls in the white region center which is very close to the one for pure white light (0.33, 0.33). The white light originated from the trichromatic superposition of the blue light-emitting PPV derivative, red light-emitting CdSe/ZnS NCs and green light-emitting metal complex of MQ units formed on surface of the NCs.

In order to clearly understand the effect of MQ on the PL properties of NCs in polymer matrix, we also measured the PL spectra of P-NCs/MQ (10:1), P-NCs/MQ (5:1) and P-NCs/MQ (1:1) (Fig. 12). It can be seen that there are two emission centers, including the inherent luminescent emission of NCs at 625 nm and the metal complexes (ZnMQ) formed on the surface of NCs at about 500 nm. With the increasing ratio of MQ to NCs, the characteristic emission of NCs is gradually suppressed, while the PL intensities of ZnMQ complexes are increased and the emission peaks are red-shifted. Especially, for the P-NCs/MQ (1:1), the PL intensity of ZnMQ complex on NCs is higher than that the inherent emission of NCs. However, with the increasing content of MQ in polymer matrices, the luminescent intensities of the bulk nanocomposites decrease on the whole. The fluorescence quenching of bulk nanocomposites is possibly caused by the charge separation from the NCs to the metal complexes (ZnMQ) formed on the surface of NCs.

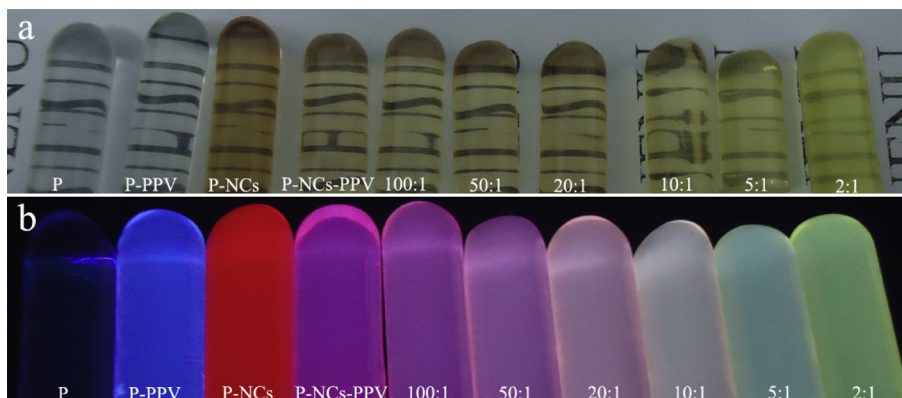
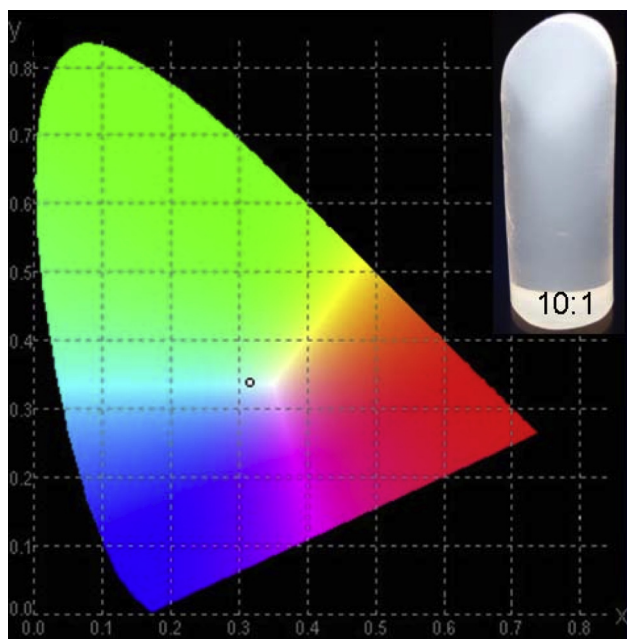


Fig. 10. Optical photograph of different polymer samples under (a) daylight and (b) under a UV lamp of 365 nm.



**Fig. 11.** CIE chromaticity diagram for P-NCs/MQ(10:1)-PPV. Inset: the photograph of P-NCs/MQ(10:1)-PPV under excitation at 365 nm with a UV lamp.

There are two main charge transfer (CT) processes that are thermodynamically favorable based on the valence and conduction band energies of the NCs and ZnMQ [51]. In the first case, a hole is transferred from the NCs to the ZnMQ complex following NCs photoexcitation. And in another case, the electron is injected into the conduction band of the NCs following photoexcitation of the ZnMQ complex. It has been demonstrated that the charge transfer rate in NCs/conjugated polymer hybrids can be controlled by using a series of core/shell QDs with varying shell thickness [52]. Thus, by changing the NCs chemical constituents with suitable control of the core and shell material and size, it should be possible to prevent charge transfer process and keep the original emission of NCs. Further study is needed to better understand the CT mechanism between the core–shell NCs and the metal complex generated on the surface of NCs in the unique and interesting nanosystems.

The thermal stabilities of the pure polymer matrix and the bulk nanocomposites of P-NCs/MQ(10:1)-PPV and P-NCs/MQ(2:1)-PPV were studied and their TGA curves are shown in Fig. 13. The

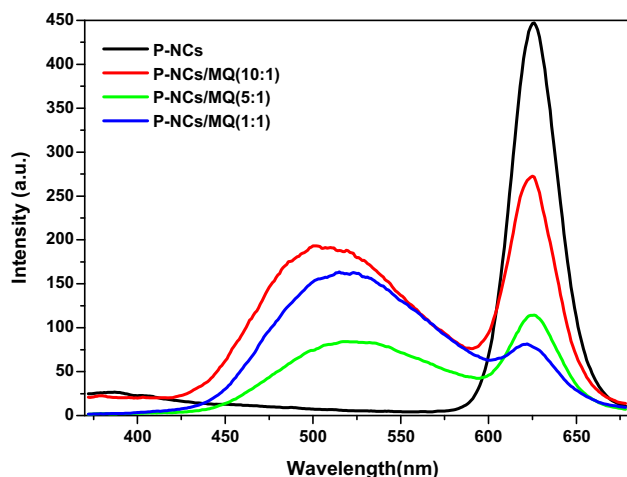


**Fig. 12.** PL spectra of P-NCs, P-NCs/MQ(10:1), P-NCs/MQ(5:1) and P-NCs/MQ(1:1).

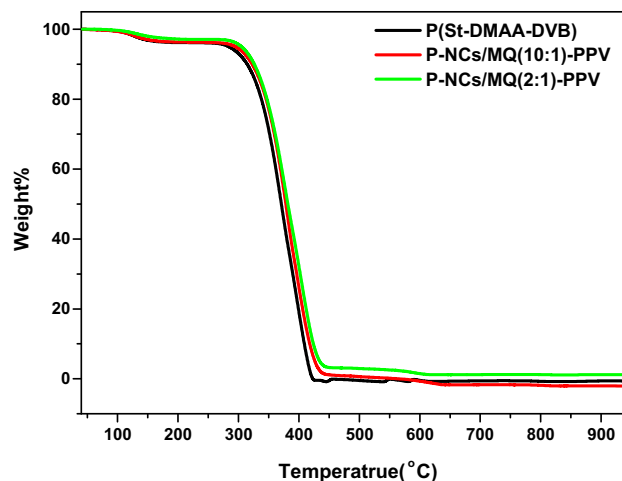


**Fig. 13.** TGA curves of polymer matrix, P-NCs/MQ(10:1)-PPV and P-NCs/MQ(2:1)-PPV.

nanocomposites exhibit the similar TGA profiles as the pristine polymer matrix. The initial weight losses of 4–5% between 110 and 200 °C correspond to the weight loss of the adsorbed water and unreacted organic monomers. The obvious weight losses above 280 °C are attributed to the decomposition of the polymer matrix, and the nanocomposites have completely decomposed above 430 °C. So the nanocomposites still preserve the good thermal stability due to the low addition weight (about 0.4 wt%) of NCs.

#### 4. Conclusions

The new functionalized conjugated/non-conjugated MEH-PPV derivatives containing MEH-PPV moieties, VBCPPX moieties and VBPPX moieties have been synthesized via a *p*-quinodimethane intermediate route. The styrene group and carboxyl group were simultaneously incorporated into the side chains of the polymer by a one-pot route under a mild condition. This novel synthetic strategy is more facile than those traditional synthetic methods. The synthesized MEH-PPV derivatives, CdSe/ZnS NCs and functional ligand (MQ) have been successfully integrated into the polymer matrix by *in situ* polymerization to fabricate a series of transparent bulk fluorescent nanocomposites. The covalent bonding linkage between the different components including MQ decorated NCs, MEH-PPV derivatives and polymer matrix could prevent phase separation between the NCs and polymers, and endow the resultant nanocomposites with good transparency and stable fluorescent properties. Our method can also provide a facile strategy for preparing white light emitting polymer nanocomposites by easily adjusting the ratio of different components. We anticipate that this method would provide a platform for the fabrication of diverse fluorescent polymer nanocomposites, which would have the potential applications in fabricating multifunctional devices with special optical, electrical, and other properties.

#### Acknowledgments

This work was supported by the National Natural Science Foundation of China (21074019) and Natural Science Foundation of Jilin Province (20101539).

#### Appendix A. Supplementary data

Supplementary data related to this article can be found at <http://dx.doi.org/10.1016/j.dyepig.2013.04.038>.

## References

- [1] Lü X, Yang J, Fu Y, Liu Q, Qi B, Lü C, et al. White light emission from Mn<sup>2+</sup> doped ZnS nanocrystals through the surface chelating of 8-hydroxyquinoline-5-sulfonic acid. *Nanotechnology* 2010;21:115702.
- [2] Zhang X, Mohandessi S, Miller LW, Snee PT. Efficient functionalization of aqueous CdSe/ZnS nanocrystals using small-molecule chemical activators. *Chem Commun* 2011;47:3532–4.
- [3] Henglein A. Small-particle research: physicochemical properties of extremely small colloidal metal and semiconductor particles. *Chem Rev* 1989;89:1861–73.
- [4] Weller H. Colloidal semiconductor Q-particles: chemistry in the transition region between solid state and molecules. *Angew Chem Int Ed Engl* 1993;32:41–53.
- [5] Alivisatos AP. Perspectives on the physical chemistry of semiconductor nanocrystals. *J Phys Chem* 1996;100:13226–39.
- [6] Peng XG, Manna L, Yang WD, Wickham J, Scher E, Kadavanich A, et al. Shape control of CdSe nanocrystals. *Nature* 2000;404:59–61.
- [7] Coe S, Woo WK, Bawendi M, Bulović V. Electroluminescence from single monolayers of nanocrystals in molecular organic devices. *Nature* 2002;420:800–3.
- [8] Achermann M, Petruska MA, Kos S, Smith DL, Koleske DD, Klimov VI. Energy-transfer pumping of semiconductor nanocrystals using an epitaxial quantum well. *Nature* 2004;429:642–6.
- [9] Medintz IL, Clapp AR, Mattoussi H, Goldman ER, Fisher B, Mauro JM. Self-assembled nanoscale biosensors based on quantum dot FRET donors. *Nat Mater* 2003;2:630–8.
- [10] Chan WCW, Nie S. Quantum dot bioconjugates for ultrasensitive nonisotopic detection. *Science* 1998;281:2016–8.
- [11] (a) Zhang H, Cui Z, Wang Y, Zhang K, Ji X, Lu C, et al. From water-soluble CdTe nanocrystals to fluorescent nanocrystal-polymer transparent composites using polymerizable surfactants. *Adv Mater* 2003;15:777–80; (b) Wei H, Sun H, Zhang H, Gao C, Yang B. An effective method to prepare polymer/nanocrystal composites with tunable emission over the whole visible light range. *Nano Res* 2010;3:496–505; (c) Sun H, Zhang H, Zhang J, Wei H, Ju J, Li M, et al. White-light emission nanofibers obtained from assembling aqueous single-colored CdTe NCs into a PPV precursor and PVA matrix. *J Mater Chem* 2009;19:6740–4.
- [12] Lee, Sundar VC, Heine JR, Bawendi MG, Jensen KF. Full color emission from II–VI semiconductor quantum dot–polymer composites. *Adv Mater* 2000;12:1102–5.
- [13] Pang L, Shen YM, Tetz K, Fainman Y. PMMA quantum dots composites fabricated via use of pre-polymerization. *Opt Express* 2005;13:44–9.
- [14] Lü C, Gao J, Fu Y, Du Y, Shi Y, Su Z. A ligand exchange route to highly luminescent surface-functionalized ZnS nanoparticles and their transparent polymer nanocomposites. *Adv Funct Mater* 2008;18:3070–9.
- [15] Gao J, Lü C, Lü X, Du Y. APhen-functionalized nanoparticles/polymer fluorescent nanocomposites via ligand exchange and in-situ bulk polymerization. *J Mater Chem* 2007;17:4591–7.
- [16] Althues H, Palkovits R, Rumpelcker A, Simon P, Sigle W, Bredol M, et al. Synthesis and characterization of transparent luminescent ZnS: Mn/PMMA nanocomposites. *Chem Mater* 2006;18:1068–72.
- [17] Hung CH, Whang WT. Effect of surface stabilization of nanoparticles on luminescent characteristics in ZnO/poly(hydroxyethyl methacrylate) nanohybrid films. *J Mater Chem* 2005;15:267–74.
- [18] Burroughes JH, Bradley DDC, Brown AR, Marks RN, MacKay K, Friend RH, et al. Light-emitting diodes based on conjugated polymers. *Nature* 1990;347:539–41.
- [19] (a) Jin S, Kim M, Kim JY, Lee K, Gal Y. High-efficiency poly(p-phenylenevinylene)-based copolymers containing an oxadiazole pendant group for light-emitting diodes. *J Am Chem Soc* 2004;126:2474–80; (b) He F, Xia H, Tang S, Duan Y, Zeng M, Liu L, et al. A novel amorphous oligo(phenylenevinylene) dimer with a biphenyl linkage center and fluorene end groups for electroluminescent devices. *J Mater Chem* 2004;14:2735–40.
- [20] Bente H, Ogawa M, Ohkita H, Ito S. Design of multilayered nanostructures and donor-acceptor interfaces in solution-processed thin-film organic solar cells. *Adv Funct Mater* 2008;18:1563–72.
- [21] Zhao D, Du J, Chen Y, Ji X, He Z, Chan W. A quencher-tether-ligand probe and its application in biosensor based on conjugated polymer. *Macromolecules* 2008;41:5373–86.
- [22] Lipomi DJ, Chiechi RC, Reus WF, Whitesides GM. Laterally ordered bulk heterojunction of conjugated polymers: nanoskiving a jelly roll. *Adv Funct Mater* 2008;18:3469–77.
- [23] Fang J, Matyba P, Robinson ND, Edman L. Identifying and alleviating electrochemical side-reactions in light-emitting electrochemical cells. *J Am Chem Soc* 2008;130:4562–8.
- [24] Duncan TV, Park S. A new family of color-tunable light-emitting polymers with high quantum yields via the controlled oxidation of MEH-PPV. *J Phys Chem B* 2009;113:13216–21.
- [25] Zhang J, Gao G, Dong W, Zhao D, Liu F. Polychromatic light-emitting conjugated polymer prepared by controlling its structure through active free radical addition. *Polym Int* 2008;57:921–6.
- [26] (a) Yang CH, He GF, Wang RQ, Li YF. Synthesis and electrochemical characterization of soluble poly(p-phenylene vinylene) derivatives containing olefinic bonds at the side chain. *J Appl Polym Sci* 1999;73:2535–9; (b) Yang C, Hou J, Zhang B, Zhang S, He C, Fang H, et al. Electroluminescent and photovoltaic properties of the crosslinkable poly(phenylene vinylene) derivative with side chains containing vinyl groups. *Macromol Chem Phys* 2005;206:1311–8.
- [27] Kubo M, Takimoto C, Minami Y, Uno T, Itoh T. Incorporation of  $\pi$ -conjugated polymer into silica: preparation of poly[2-methoxy-5-(2-ethylhexyloxy)-1,4-phenylenevinylene]/silica and poly(3-hexylthiophene)/silica composites. *Macromolecules* 2005;38:7314–20.
- [28] Duchateau J, Lutsen L, Guedens W, Cleij TJ, Vanderzande D. Versatile post-polymerization functionalization of poly(p-phenylene vinylene) copolymers containing carboxylic acid substituents: development of a universal method towards functional conjugated copolymers. *Polym Chem* 2010;1:1313–22.
- [29] Kang J, Cho H, Lee J, Lee S, Cho N, et al. Highly bright and efficient electroluminescence of new PPV derivatives containing polyhedral oligomeric silsesquioxanes (POSSs) and their blends. *Macromolecules* 2006;39:4999–5008.
- [30] Jin S, Jung H, Hwang C, Koo D, Shin W, Kim Y, et al. High electroluminescent properties of conjugated copolymers from poly[9,9-dioctylfluorenyl-2,7-vinylene]-co-(2-(3-dimethyldodecylsilylphenyl)-1,4-phenylenevinylene)] for light-emitting diode applications. *J Polym Sci Polym Chem* 2005;43:5062–71.
- [31] (a) Gu Z, Bao Y, Zhang Y, Wang M, Shen Q. Anionic water-soluble poly(phenylenevinylene) alternating copolymer: high-efficiency photoluminescence and dual electroluminescence. *Macromolecules* 2006;39:3125–31; (b) Gao Y, Wang C, Wang L, Wang H. Conjugated polyelectrolytes with pH-dependent conformations and optical properties. *Langmuir* 2007;23:7760–7; (c) Pinto MR, Schanze KS. Conjugated polyelectrolytes: synthesis and applications. *Synthesis* 2002:1293–309.
- [32] Neef CJ, Ferraris JP. MEH-PPV: improved synthetic procedure and molecular weight control. *Macromolecules* 2000;33:2311–4.
- [33] Burn PL, Kraft A, Baigent DR, Bradley DDC, Brown AR, Friend RH, et al. Chemical tuning of the electronic properties of poly(p-phenylenevinylene)-based copolymers. *J Am Chem Soc* 1993;115:10117–24.
- [34] Ahn T, Shim HK. Synthesis and luminescent properties of blue light emitting polymers containing both hole and electron transporting units. *Macromol Chem Phys* 2001;202:3180–8.
- [35] Lü C, Cui Z, Wang Y, Li Z, Guan C, Yang B, et al. Preparation and characterization of ZnS–polymer nanocomposite films with high refractive index. *J Mater Chem* 2003;13:2189–95.
- [36] Niu J, Shen H, Wang H, Xu W, Lou S, Du Z, et al. Investigation on the phosphine-free synthesis of CdSe nanocrystals by cadmium precursor injection. *New J Chem* 2009;33:2114–9.
- [37] Yu WW, Qu L, Guo W, Peng X. Experimental determination of the extinction coefficient of CdTe, CdSe, and CdS nanocrystals. *Chem Mater* 2003;15:2854–60.
- [38] Shen H, Wang H, Tang Z, Niu J, Lou S, Du Z, et al. High quality synthesis of monodisperse zinc-blende CdSe and CdSe/ZnS nanocrystals with a phosphine-free method. *CrystEngComm* 2009;11:1733–8.
- [39] Cui H, Chen H, Qu R, Wang C, Ji C, Sun C, et al. Synthesis of monodisperse crosslinked polystyrene microspheres via dispersion copolymerization with the crosslinker-postaddition method. *J Appl Polym Sci* 2008;107:3909–16.
- [40] Wu X, Shi G, Chen F, Han S, Peng J. High-quality poly[2-methoxy-5-(2'-ethylhexyloxy)-p-phenylenevinylene] synthesized by a solid–liquid two-phase reaction: characterizations and electroluminescence properties. *J Polym Sci Pol Chem* 2004;42:3049–54.
- [41] Yang SH, Wu CC, Lee CF, Liu MH. Synthesis and luminescence of red MEH-PPV: P3OT polymer. *Displays* 2008;29:214–8.
- [42] Peppas NA, Wright SL. Drug diffusion and binding in ionizable interpenetrating networks from poly(vinyl alcohol) and poly(acrylic acid). *Eur J Pharm Biopharm* 1998;46:15–29.
- [43] Kurkuri MD, Aminabhavi TM. Poly(vinyl alcohol) and poly(acrylic acid) sequential interpenetrating network pH-sensitive microspheres for the delivery of diclofenac sodium to the intestine. *J Control Release* 2004;96:9–20.
- [44] Fan Y, Lin K. Dependence of the luminescent properties and chain length of poly[2-methoxy-5-(2'-ethyl-hexyloxy)-1,4-phenylene vinylene] on the formation of cis-vinylene bonds during Gilch polymerization. *J Polym Sci Pol Chem* 2005;43:2520–6.
- [45] (a) Zhang R, Tang J, Zhang G, Shen J. A new kind of copolymerization of styrene and p-quinodimethane intermediates. *Macromol Rapid Commun* 2001;22:383–5; (b) Tang J, Zhang R, Li G, Shen J. Novel blue light emitting copolymer with both conjugated and nonconjugated segments. *Chem Mater* 2003;15:2950–3.
- [46] Wagaman MW, Grubbs RH. Synthesis of organic and water soluble poly(1,4-phenylenevinylenes) containing carboxyl groups: living ring-opening metathesis polymerization (ROMP) of 2,3-dicarboxybarrelenes. *Macromolecules* 1997;30:3978–85.
- [47] Gavrilko T, Fedorovich R, Dovbeshko G, Marchenko A, Naumovets A, Nechytaylo V, et al. FTIR spectroscopic and STM studies of vacuum deposited aluminum (III) 8-hydroxyquinoline thin films. *J Mol Struct* 2004;704:163–8.
- [48] Koole R, Lijeroth P, Donegá CM, Vanmaekelbergh D, Meijerink A. Electronic coupling and exciton energy transfer in CdTe quantum-dot molecules. *J Am Chem Soc* 2006;128:10436–41.
- [49] Althues H, Henle J, Kaskel S. Functional inorganic nanofillers for transparent polymers. *Chem Soc Rev* 2007;36:1454–65.
- [50] Lü C, Cheng Y, Liu Y, Liu F, Yang B. A facile route to ZnS/polymer nanocomposite optical materials with high nanophase contents via  $\gamma$ -ray irradiation-initiated bulk polymerization. *Adv Mater* 2006;18:1188–92.
- [51] Sykora M, Petruska MA, Alstrum-Acevedo J, Bezel I, Meyer TJ, Klimov VI. Photoinduced charge transfer between CdSe nanocrystal quantum dots and Ru–polypyridine complexes. *J Am Chem Soc* 2006;128:9984–5.
- [52] Xu ZH, Hine CR, Maye MM, Meng QP, Cotlet M. Shell thickness dependent photoinduced hole transfer in hybrid conjugated polymer/quantum dot nanocomposites: from ensemble to single hybrid level. *ACS Nano* 2012;6:4984–92.